DØnote 4387

Search for the Higgs boson $H \to WW^{(*)} \to l^+\nu l'^-\bar{\nu}$ $(l, l' = e, \mu)$ decays at DØ in Run II

The DØ Collaboration
URL: http://www-d0.fnal.gov

(Dated: March 24, 2004)

This document describes the search for the Higgs boson in the channels $H \to WW^{(*)} \to l^+\nu l'^-\bar{\nu}$ $(l = e, \mu)$ at DØ with data taken between April 2002 and September 2003 corresponding to an integrated luminosity up to $\mathcal{L} \approx 147 - 177\,\mathrm{pb}^{-1}$ depending on the final state. The number of events observed is consistent with expectations from standard model backgrounds. Limits from the combination of the ee, $e\mu$, and $\mu\mu$ channels on the production cross section times branching ratio $\sigma \times BR(H \to WW^{(*)})$ are presented.

Preliminary Results for Winter 2004 Conferences

I. INTRODUCTION

This note describes the search of the Higgs boson in the channels $H \to WW^{(*)} \to e^+\nu e^-\bar{\nu}$, $H \to WW^{(*)} \to e^\pm\nu\mu^\mp\nu$ and $H \to WW^{(*)} \to \mu^+\nu\mu^-\bar{\nu}$. The final states of these processes are characterized by two isolated leptons (e or μ) with high transverse momentum p_T and a significant missing transverse energy originating from the undetected neutrinos. For further phenomenological discussions the reader is referred to [1]. It is assumed that the reader is familiar with the DØ detector [2].

Not all aspects of the analysis are discussed in detail. A description of data and Monte Carlo (MC) samples together with trigger luminosity and selection issues are presented in two separate notes. A detailed discussion of efficiencies and data and Monte Carlo comparisons can be found in [3] for the $H \to WW^{(*)} \to e^+\nu e^-\bar{\nu}$ and $H \to WW^{(*)} \to e^\pm\nu\mu^\mp\nu$ channels whereas the $H \to WW^{(*)} \to \mu^+\nu\mu^-\bar{\nu}$ channel is presented in-depth in [4].

Section II of this note describes the various data and MC samples used. Section III of this note gives an overview of the event selection in the three different channels and shows some distributions of data and Monte Carlo comparisons. Section IV provides a presentation of the limits on the cross section times branching ratio $\sigma \times BR(H \to WW)$ for the combination of all three channels.

II. DATA AND MONTE CARLO SAMPLES

This analysis uses data collected by the DØ experiment between April 2002 and September 2003. The total integrated luminosity of the sample is in the range of $\mathcal{L} \approx 147 - 177\,\mathrm{pb}^{-1}$ depending on the final state. All simulated events are generated using PYTHIA 6.202 [5] and ALPGEN [6] using the CTEQ4L parton distribution function [7]. They are processed through a full detector simulation with an overlaid Poisson-distributed average of 0.8 minimum bias events. The events simulated with ALPGEN have been used for systematic studies only. The NLO cross sections for the processes $H \to WW^{(*)} \to l^+\nu l'^-\bar{\nu}$ are calculated using HDECAY [8] and HIGLU [9] with CTEQ5M parton distribution function and a top quark mass of $m_t = 175\,\mathrm{GeV}$. Table I gives an overview of all Monte Carlo samples with their cross sections and references used in comparisons with data. The contribution from QCD events was estimated from data.

III. EVENT SELECTION

A. ee-Selection

Events for the ee final state are selected by a combination of different single and dielectron triggers. At level 1 the triggers require one or two electromagnetic trigger towers above a certain p_T threshold. Typical values are 10 GeV for single electron and 5 GeV for dielectron triggers. The p_T requirement on level 3 depends on the additional requirements of the trigger under consideration. Triggers with additional shower shape or track requirements have

TABLE I: Monte Carlo samples cross sections times branching ratio and their references used in comparisons with data. The cross sections are only given for a single lepton flavor. For decays with one electron and one muon in the final state, the cross section times branching ratio must be multiplied by a factor of two.

	Process	$\sigma \times BR$ [pb]	Reference
1	$H \to WW^{(*)} \to l^+\nu l'^-\bar{\nu}$ ($M_H = 100\,\mathrm{GeV}$)	0.00012	[8],[9]
2	$H \to WW^{(*)} \to l^+\nu l'^-\bar{\nu}$ ($M_H = 120\,\mathrm{GeV}$)	0.00095	[8],[9]
3	$H \to WW^{(*)} \to l^+\nu l'^-\bar{\nu}$ ($M_H = 140\,\mathrm{GeV}$)	0.00219	[8],[9]
4	$H \to WW^{(*)} \to l^+\nu l'^-\bar{\nu}$ ($M_H = 160\,\mathrm{GeV}$)	0.00269	[8],[9]
5	$H \to WW^{(*)} \to l^+\nu l'^-\bar{\nu}$ ($M_H = 180\,\mathrm{GeV}$)	0.00189	[8],[9]
6	$H \to WW^{(*)} \to l^+\nu l'^-\bar{\nu}$ ($M_H = 200\,\mathrm{GeV}$)	0.00104	[8],[9]
7	$Z \to ll$ $(l = e, \mu, \tau)$	260	[10]
8	$WW \to l^\pm\nu l'^\mp\bar{\nu}$ $(l, l' = e, \mu)$	0.145	[11]
10	$t\bar{t} \to b\,l^\pm\nu b\,l'^\mp\bar{\nu}$ $(l, l' = e, \mu)$	0.065	[12]
11	$W(\to l)$ $(l = e, \mu)$	2800	[10]
12	$WZ(\to ll'l')$ $(l, l' = e, \mu)$	0.013	[11]
13	$\Upsilon(1s) \to ee$	1900	[5]
14	$\Upsilon(2s) \to ee$	1450	[5]

TABLE II: Summary of signal selection cuts for the ee, $e\mu$, and $\mu\mu$ channel.

	ee	$e\mu$	$\mu\mu$
cut 1	$p_T^{e1} > 12\,\text{GeV}, p_T^{e2} > 8\,\text{GeV}$ opposite charge, $N^{\text{SMT}} > 2$	$p_T^{e} > 12\,\text{GeV}, p_T^{\mu} > 8\,\text{GeV}$ opposite charge, $N^{\text{SMT}} > 2$	$p_T^{\mu 1} > 20\,\text{GeV}, p_T^{\mu 2} > 10\,\text{GeV}$ opposite charge, $N^{\text{SMT}} > 2$ $m_{\mu\mu} > 20\,\text{GeV}$
cut 2	$\not\!\!E_T > 20\,\text{GeV}$	$\not\!\!E_T > 20\,\text{GeV}$	$\not\!\!E_T > 30\,\text{GeV}$ and $\not\!\!E_T > 0.75 \cdot p_T^{\mu 1} + 10\,\text{GeV}$
cut 3	$12\,\text{GeV} < m_{ee} < 80\,\text{GeV}$	$m_T^{\min} > 20\,\text{GeV}$	$\lvert m_{\mu\mu} - M_Z \rvert > 15\,\text{GeV}$
cut 4	$p_T^{e_1} + p_T^{e_2} + \not\!\!E_T > 100\,\text{GeV}$	$p_T^{e} + p_T^{\mu} + \not\!\!E_T > 90\,\text{GeV}$	$\Delta\phi_{\mu\mu} < 2.0$
cut 5	$\Delta\phi_{ee} < 1.5$	$\Delta\phi_{e\mu} < 2.0$	No jet or ($E_T^{Jet1} < 60\,\text{GeV}$ and $E_T^{Jet2} < 30\,\text{GeV}$)
cut 6	$\not\!\!E_T{}^{scaled} > 15\sqrt{\text{GeV}}$	$\not\!\!E_T{}^{scaled} > 15\sqrt{\text{GeV}}$	
cut 7	No jet or $E_T^{Jet1} < 90\,\text{GeV}$ or $E_T^{Jet1} < 50\,\text{GeV}$ and $E_T^{Jet2} < 30\,\text{GeV}$	No jet or $E_T^{Jet1} < 90\,\text{GeV}$ or $E_T^{Jet1} < 50\,\text{GeV}$ and $E_T^{Jet2} < 30\,\text{GeV}$	

low p_T thresholds at 12 GeV whereas the threshold without any additional requirement is at 30 GeV. The integrated luminosity for a combination of all triggers corresponds to $177 \pm 12\,\text{pb}^{-1}$.

The electrons must pass shower shape and likelihood criteria. The likelihood criterion includes a track match for all electrons and uses an E/p requirement for electrons in the central region. The leading electron should have $p_T > 12\,\text{GeV}$, the second electron $p_T > 8\,\text{GeV}$. The electrons should come from the same vertex and should have opposite charge. To reject electrons from conversions, the trailing electron should have at least three hits in the silicon tracker detector. Events that passed the preselection (cut 1) are then required to have a missing transverse energy of $\not\!\!E_T > 20\,\text{GeV}$ (cut 2). To reject contributions from resonance decays the invariant dielectron mass should be $12\,\text{GeV} < m_{ee} < 80\,\text{GeV}$ (cut 3). The sum of the electron momenta and the missing transverse energy is expected to be small for Drell-Yan decays and $W + jet$ events. Requiring $p_T^{e_1} + p_T^{e_2} + \not\!\!E_T > 100\,\text{GeV}$ rejects most of these events (cut 4). Remaining Z boson and multi-jet events can be rejected with a cut on the opening angle $\Delta\phi_{ee}$, since most of the background decays are back-to-back. This is not the case for Higgs boson decays because of the spin correlations in the decay. The cut is applied at $\Delta\phi_{ee} < 1.5$ (cut 5). Remaining events from Z boson decays are characterized by a small opening angle between the electrons and large missing transverse energy. The small opening angle arises from a large boost of the Z boson caused by one or more jets. A mismeasurement of these jets is a likely source for the missing transverse energy in the event. The events can be tested if the missing transverse energy is generated by a mismeasurement of the jet. The scaled missing transverse energy is defined as $\not\!\!E_T{}^{scaled} = \frac{\not\!\!E_T}{\sqrt{E_{jet}} \cdot \sin\Theta_{jet} \cdot \lvert\cos(\Delta\phi(jet, \not\!\!E_T))\rvert}$. Requiring $\not\!\!E_T{}^{scaled} > 15\sqrt{\text{GeV}}$ is expected to remove those events (cut 6). Contributions from $t\bar{t}$ events can be reduced with a jet veto criterion. If one jet is found in the event, the E_T of the jet has to be less than 90 GeV. For events with two or more jets the leading jet must have $E_T^{Jet1} < 50\,\text{GeV}$, the second leading jet $E_T^{Jet2} < 30\,\text{GeV}$ (cut 7). Table II summarizes all selection criteria for the ee final state.

In Table III the predictions from the Monte Carlo are compared with the events observed in the data after every step of the selection. After the final selection two events remain in the data while 2.7 ± 0.4 events are expected from backgrounds. The expected number of events for a standard model Higgs boson of mass $M_H = 160$ GeV is 0.073 ± 0.002 events. The signal efficiencies depend strongly on the Higgs boson mass and are between $(2.3 \pm 0.2)\%$ ($M_H = 100$ GeV) and $(15.5 \pm 0.4)\%$ ($M_H = 160$ GeV). The efficiencies after the final selection are shown for all Higgs boson masses in Table IV. Figure 1 shows the distribution of the opening angle between the leptons $\Delta\phi$ after cut 1 (left) and all cuts 1–7 (right) and invariant mass after cut 1–2 (bottom).

B. $e\mu$-Selection

Events are selected using different electron muon triggers. Like in the ee channel, the p_T thresholds of the electron triggers depend on the requirements on the electron quality. The p_T thresholds for the trigger towers at level 1 range between 3 and 6 GeV. At level 3, the electron must have p_T greater than 10 or 12 GeV (depending on the trigger-list), with an additional shower shape criterion the threshold is lowered to 7 GeV. The muon trigger requires one tight scintillator muon object at level 1. The luminosity of the combination of these triggers is found to be

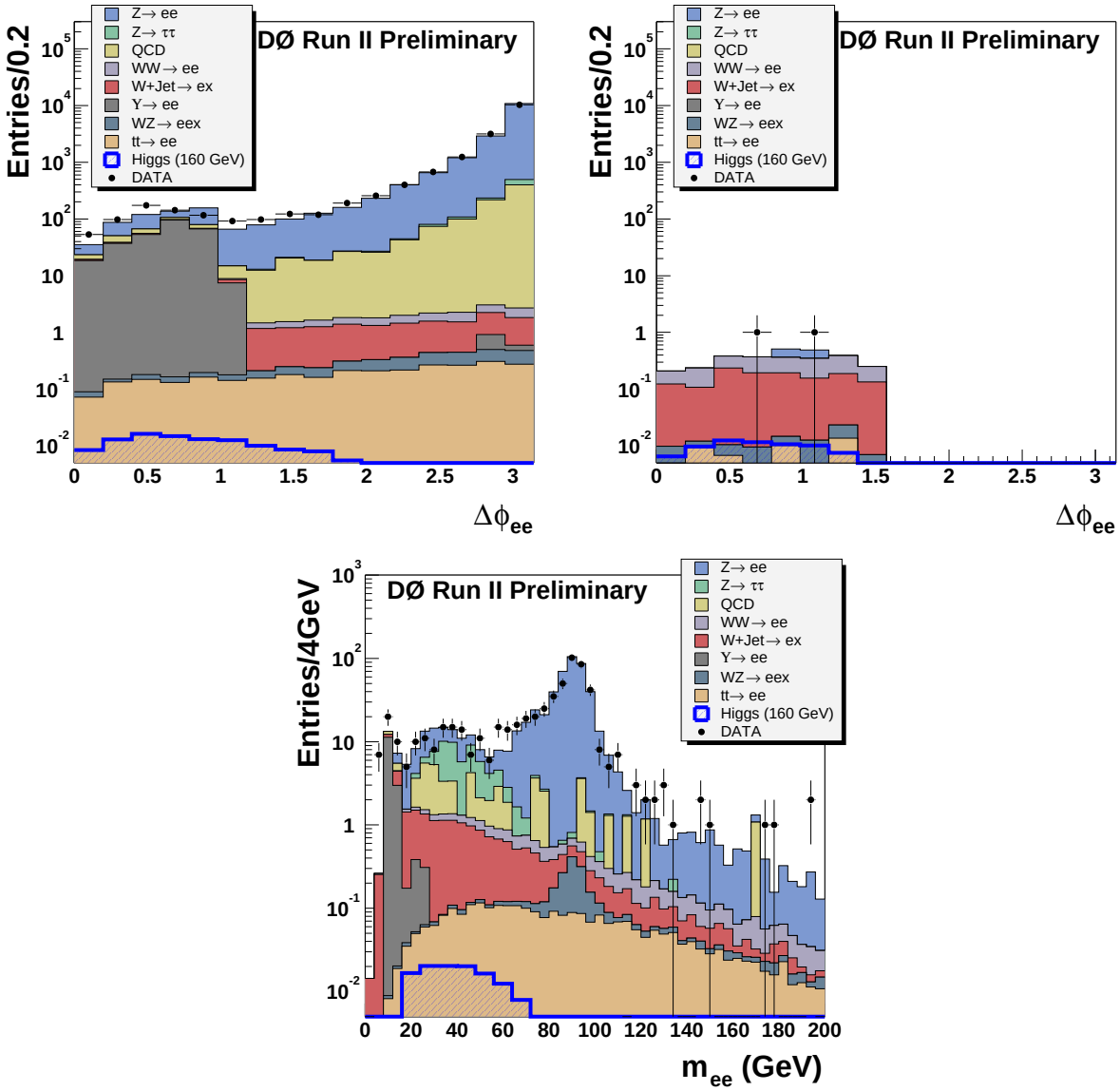

FIG. 1: Distribution of the opening angle between the leptons $\Delta\phi$ for the ee channel after cut 1 (left) and cut 1–7 (right) and invariant mass after cut 1–2 (bottom). The Monte Carlo is normalized to the integrated luminosity in the data.

$\mathcal{L} = 158 \pm 10\,\mathrm{pb}^{-1}$.

The event selection is similar to that in the ee channel. The electrons have to satisfy the same identification criteria and the track of the electron must have at least three hits in the silicon tracker. The electron p_T is required to be in excess of 12 GeV. The muon must pass 'medium' muon criteria and should have a track in the tracker. The muon quality criterion is defined by a combination of hits in the wire chambers and scintillators of the muon system. A muon is called "medium" if it has at least two hits in the A layer wire chambers, at least one hit in the A layer scintillator, at least two hits in the BC layer wire chambers and at least one hit in the BC scintillator (except for central muons with less than four BC wire hits). Track isolation ($\sum_{tracks}^{\Delta\mathcal{R}<0.5} p_T < 2.5\,\mathrm{GeV}$) and calorimeter isolation criteria ($E(\Delta\mathcal{R} < 0.4) - E(\Delta\mathcal{R} < 0.1) < 2.5\,\mathrm{GeV}$) are applied. A scintillator timing cut in the A and BC layer is used to reject muons from cosmic radiation. The p_T of the muon is required to be greater than 8 GeV (cut 1).

To enhance signal with respect to background a cut on the missing transverse energy is applied. The criterion is $\not\!\!E_T > 20\,\mathrm{GeV}$ (cut 2). Instead of the invariant mass cut, a cut on the minimal transverse mass $\sqrt{2 \cdot \not\!\!E_T \cdot p_T \cdot (1 - \cos(\Delta\phi))}$ is applied. Requiring $\min(m_T^e, m_T^\mu) > 20\,\mathrm{GeV}$ (cut 3) rejects a large fraction of the $Z/\gamma^* \to \tau^+\tau^-$ decays. The sum of the lepton transverse momenta and the missing transverse energy must be greater than 90 GeV (cut 4). Using again the spin correlations in the Higgs boson decay, a cut on the opening angle between the two leptons is applied at

TABLE III: Cut flow table for the ee channel. The quoted errors are statistical only.

	$t\bar{t} \to be^+\nu be^-\bar{\nu}$	$WZ \to e^+e^- + X$	$\Upsilon \to e^+e^-$	$W + jets$	$WW \to e^+\nu e^-\bar{\nu}$
cut 1	3.05 ± 0.05	1.48 ± 0.03	280.1 ± 6.2	18.3 ± 0.3	6.84 ± 0.06
cut 2	2.89 ± 0.05	1.33 ± 0.03	11.2 ± 1.3	16.6 ± 0.2	5.82 ± 0.05
cut 3	1.31 ± 0.03	0.14 ± 0.01	2.4 ± 0.5	13.3 ± 0.2	3.19 ± 0.04
cut 4	0.84 ± 0.03	0.10 ± 0.01	0.0 ± 0.01	3.2 ± 0.1	2.03 ± 0.03
cut 5	0.51 ± 0.02	0.05 ± 0.01	0.0 ± 0.01	1.43 ± 0.07	1.20 ± 0.02
cut 6	0.36 ± 0.02	0.05 ± 0.01	0.0 ± 0.01	1.33 ± 0.07	1.19 ± 0.02
cut 7	0.06 ± 0.01	0.04 ± 0.01	0.0 ± 0.01	1.24 ± 0.07	1.17 ± 0.02

	$Z/\gamma^* \to \tau^+\tau^-$	$Z/\gamma^* \to e^+e^-$	QCD	Total Sum	DATA
cut 1	133.6 ± 4.4	15895 ± 47	972 ± 31	17311 ± 57	17274
cut 2	36.3 ± 2.3	488 ± 8	38 ± 6	600 ± 11	602
cut 3	35.6 ± 2.3	93.0 ± 3.6	26.0 ± 5.1	175.0 ± 6.7	188
cut 4	2.9 ± 0.6	14.7 ± 1.5	4.0 ± 2.0	27.8 ± 2.6	23
cut 5	0.6 ± 0.3	4.3 ± 0.8	1.0 ± 1.0	9.1 ± 1.3	8
cut 6	0.0 ± 0.3	0.3 ± 0.1	0.0 ± 1.0	3.2 ± 1.0	3
cut 7	0.0 ± 0.1	0.1 ± 0.1	0.0 ± 0.5	2.7 ± 0.4	2

TABLE IV: Signal efficiencies with statistical error after all cuts for the ee, $e\mu$, and $\mu\mu$ channel for different Higgs boson masses M_H.

M_H [GeV]	100	120	140	160	180	200
ee	0.023 ± 0.002	0.077 ± 0.003	0.104 ± 0.003	0.155 ± 0.004	0.151 ± 0.004	0.118 ± 0.003
$e\mu$	0.014 ± 0.001	0.059 ± 0.002	0.094 ± 0.003	0.131 ± 0.004	0.137 ± 0.004	0.130 ± 0.004
$\mu\mu$	0.045 ± 0.002	0.110 ± 0.003	0.150 ± 0.004	0.216 ± 0.005	0.179 ± 0.005	0.151 ± 0.004

$\Delta\phi_{e\mu} < 2.0$ (cut 5). To remove remaining $Z/\gamma^* \to \tau^+\tau^-$, $t\bar{t}$ and multi-jet events, similar cuts on the scaled missing transverse energy ${\not\!\!E_T}^{scaled} > 15\sqrt{\text{GeV}}$ (cut 6) and on jets (cut 7) are applied. A summary of all selection criteria can be found in Table II.

Table V gives an overview on the number of expected and observed events for every step of the selection. The expectations from standard model backgrounds is in good agreement with the data. At the end of the selection, two events remain in the data, the Monte Carlo predicts 3.1 ± 0.3 events. The expected contribution for a standard model Higgs boson of mass $M_H = 160$ GeV is 0.111 ± 0.004 events. Signal efficiencies range from $(1.4 \pm 0.1)\%$ ($M_H = 100$ GeV) to $(13.7 \pm 0.4)\%$ ($M_H = 180$ GeV) depending on the Higgs boson mass. Efficiencies after the final selection for all Higgs boson masses are presented in Table IV. In Fig. 2 the opening angle between the leptons is shown at the beginning of the selection (left) and after application of cuts 1–7 (right).

C. $\mu\mu$-Selection

Events that pass the $\mu\mu$ selection should be triggered by one of four dimuon triggers that have muon requirements at the trigger level 1 and 2. Two triggers have additional track requirements at the trigger level 3. The luminosity of this sample is $\mathcal{L} \approx 147 \pm 10\,\text{pb}^{-1}$. All events should have at least two muons tracks of 'loose' quality and should be matched to their corresponding tracks in the central tracking system. A "loose" muon is defined as a medium muon (cf. Section III B) but allowing one of the medium muon tests to fail, with the A layer wire chamber and scintillator requirement treated as one test and requiring always at least one scintillator hit. The leading muon should have a transverse momentum $p_T^{\mu 1} > 20\,\text{GeV}$, the second muon should have a transverse momentum $p_T^{\mu 2} > 10\,\text{GeV}$. In addition both muons must fulfil the tracking isolation criteria, i.e. $\sum_{tracks}^{\Delta\mathcal{R}<0.5} p_T < 4.0\,\text{GeV}$ (sum of the p_T of tracks in a cone $\Delta\mathcal{R} < 0.5$ around the muon except the muon track). To reject cosmics a cut on the scintillator times in the A and BC layer of the muon system is made. To assure good quality of the muons the tracks should have at least three hits in the SMT detector and should have a distance of closest approach with respect to the nominal vertex of less than 0.15 cm. If these tracks have opposite charge and have an invariant dimuon mass $m_{\mu\mu} > 20\,\text{GeV}$ they fulfil the preselection (cut 1). The second cut requires the missing transverse energy ${\not\!\!E_T}$ in the event to be greater than 30 GeV. To avoid overestimation of ${\not\!\!E_T}$ by the leading muon track the following is required: ${\not\!\!E_T} > 0.75 \cdot p_T^{\mu 1} + 10\,\text{GeV}$.

TABLE V: Cut flow table for the $e\mu$ channel. The quoted errors are statistical only.

	$t\bar{t} \to be^{\pm}\nu b\mu^{\mp}\bar{\nu}$	$WZ \to e^{\pm}\mu^{\mp} + X$	$W + jets$	$WW \to e^{\pm}\nu\mu^{\mp}\bar{\nu}$	$Z/\gamma^* \to \tau^+\tau^-$
cut 1	3.98 ± 0.08	0.34 ± 0.01	7.2 ± 0.1	10.28 ± 0.09	168.5 ± 4.7
cut 2	3.61 ± 0.07	0.28 ± 0.01	5.0 ± 0.1	7.79 ± 0.08	27.5 ± 1.8
cut 3	2.86 ± 0.06	0.23 ± 0.01	4.2 ± 0.1	6.96 ± 0.08	2.4 ± 0.5
cut 4	2.80 ± 0.06	0.21 ± 0.01	1.41 ± 0.06	5.85 ± 0.07	1.3 ± 0.4
cut 5	1.55 ± 0.05	0.13 ± 0.01	0.94 ± 0.05	3.31 ± 0.05	0.6 ± 0.3
cut 6	0.64 ± 0.03	0.11 ± 0.01	0.35 ± 0.02	2.52 ± 0.05	0.3 ± 0.2
cut 7	0.13 ± 0.01	0.11 ± 0.01	0.34 ± 0.02	2.51 ± 0.05	0.0 ± 0.1

	$Z/\gamma^* \to \mu^+\mu^-$	QCD	Total Sum	DATA
cut 1	5.2 ± 0.8	25.2 ± 2.4	220.8 ± 5.3	218
cut 2	1.9 ± 0.5	4.2 ± 1.0	50.2 ± 2.1	54
cut 3	0.5 ± 0.2	2.3 ± 0.7	19.4 ± 1.0	21
cut 4	0.2 ± 0.1	1.6 ± 0.6	13.4 ± 0.8	12
cut 5	0.05 ± 0.05	0.9 ± 0.5	7.5 ± 0.6	6
cut 6	0.0 ± 0.05	0.0 ± 0.2	3.9 ± 0.3	4
cut 7	0.0 ± 0.05	0.0 ± 0.2	3.1 ± 0.3	2

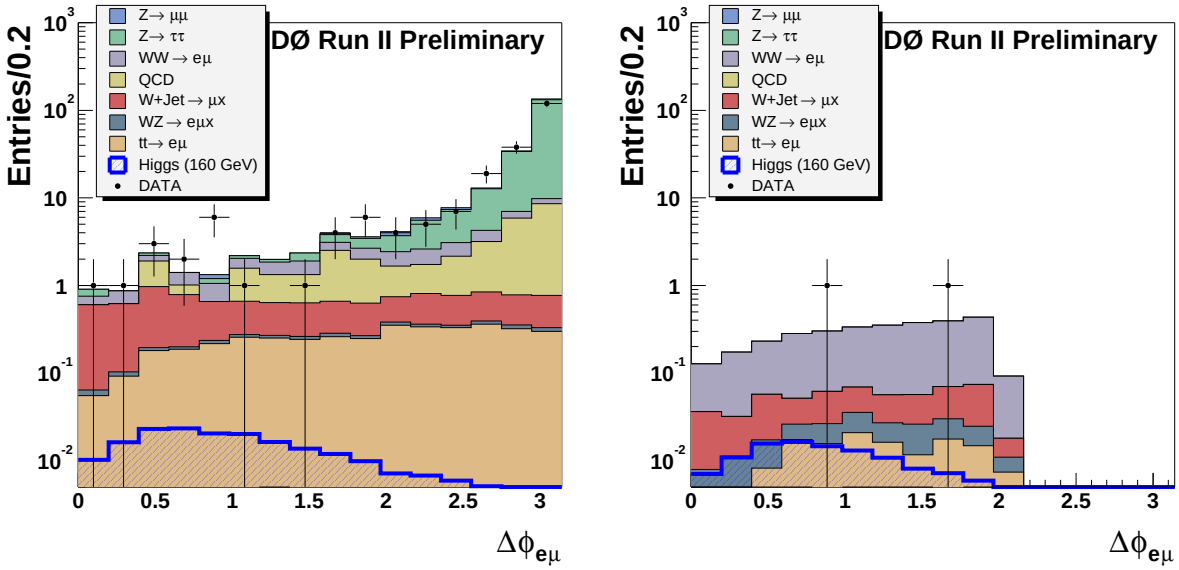

FIG. 2: Distribution of the opening angle between the leptons $\Delta\phi$ for the $e\mu$ channel after cut 1 (left) and cut 1–7 (right). The Monte Carlo is normalized to the integrated luminosity in the data.

Both latter cuts denote cut 2. To reject events from the Z resonance the invariant dimuon mass must in the range $|m_{\mu\mu} - M_Z| > 15\,\text{GeV}$ (cut 3). Since the spins from the two decaying Ws originating from the Higgs boson decay are correlated, the opening angle between the two muons tends to be smaller as compared to events from background sources. The opening angle of the two muons must therefor have $\Delta\phi_{\mu\mu} < 2.0$ (cut 4). To reject remaining events from $t\bar{t}$ and multi-jet production events are required to have zero jets or the leading jet must have $E_T^{Jet1} < 60\,\text{GeV}$ and the second jet must have $E_T^{Jet2} < 30\,\text{GeV}$ (cut 5). Table VI summarizes the cut flow described above and shows a reasonable agreement between data and Monte Carlo throughout all cuts. After applying all cuts 5 events remain in data whereas 5.3 ± 0.6 events are expected from background Monte Carlo and 0.085 ± 0.001 events are expected from a standard model $H \to WW^{(*)} \to \mu^+\nu\mu^-\bar{\nu}$ decay with a Higgs boson mass of $M_H = 160\,\text{GeV}$. The signal efficiency after all cuts ranges from $4.5 \pm 0.2\%$ for $M_H = 100\,\text{GeV}$ to a maximum of $21.6 \pm 0.5\%$ for $M_H = 160\,\text{GeV}$. Figure 3 shows the distribution of the invariant dimuon mass (top left), missing transverse energy $\not\!\!E_T$ (top right) for data and Monte Carlo after cut 1. The muon opening $\Delta\phi_{\mu\mu}$ is plotted after cut 1 (bottom left) and after all cuts 1–5 (bottom right).

Table II shows a summary of all signal selection cuts for the three different channels, whereas Table IV shows the

TABLE VI: Cut flow table for the $\mu\mu$ channel. The quoted errors are statistical only.

	$Z/\gamma^* \to \mu^+\mu^-$	QCD/W + $jets$	$Z/\gamma^* \to \tau^+\tau^-$	$WW \to \mu^+\nu\mu^-\bar{\nu}$	$t\bar{t} \to b\mu^+\nu b\mu^-\bar{\nu}$	Total Sum	DATA
cut 1	8426 ± 27	5.4 ± 0.6	57.7 ± 2.2	4.64 ± 0.05	3.15 ± 0.03	8497 ± 27	8509
cut 2	97.8 ± 2.8	1.1 ± 0.2	0.5 ± 0.2	1.98 ± 0.03	1.72 ± 0.02	103.1 ± 2.8	98
cut 3	38.8 ± 1.7	1.0 ± 0.2	0.5 ± 0.2	1.65 ± 0.03	1.34 ± 0.02	43.3 ± 1.7	53
cut 4	12.8 ± 1.0	0.2 ± 0.1	0.1 ± 0.1	1.33 ± 0.03	0.88 ± 0.01	15.3 ± 1.4	10
cut 5	3.9 ± 0.6	0.02 ± 0.02	0 ± 0	1.28 ± 0.03	0.03 ± 0.003	5.3 ± 0.6	5

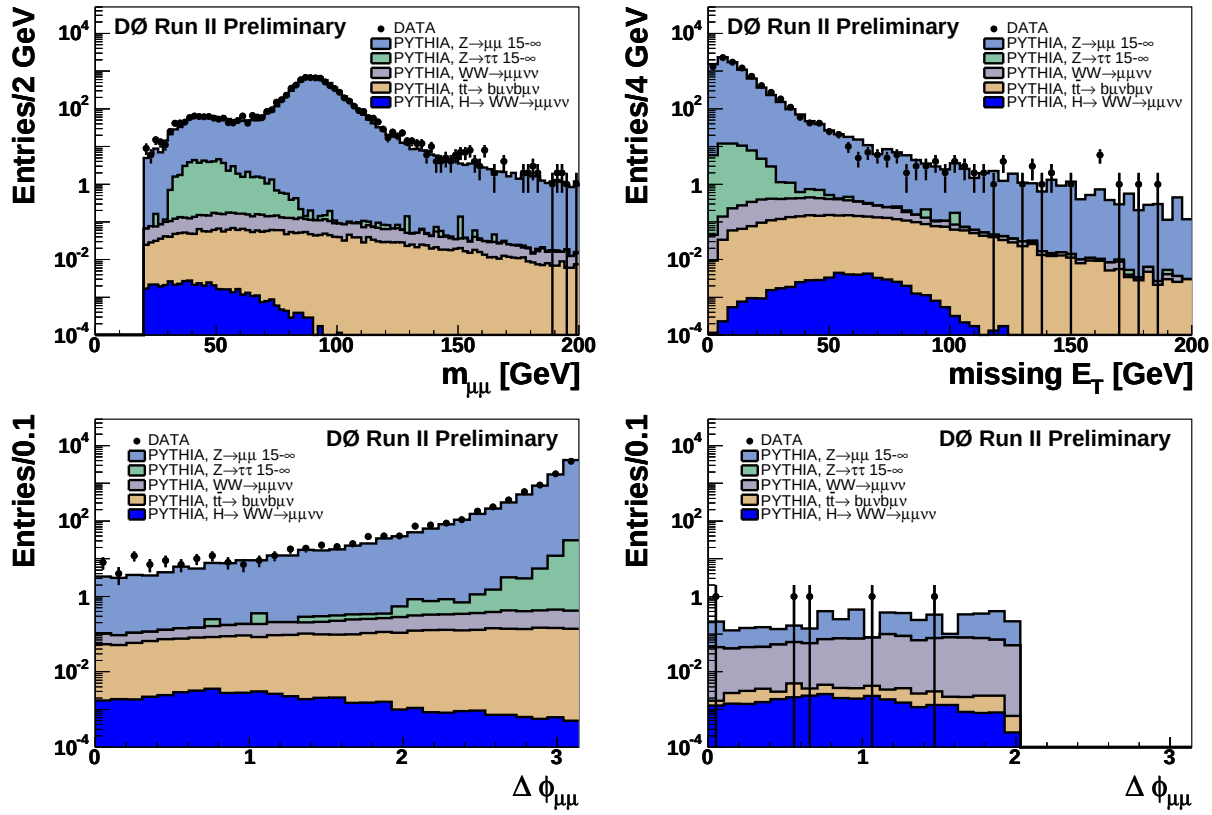

FIG. 3: Distributions for the $\mu\mu$ channel of the dimuon invariant mass $m_{\mu\mu}$ (top left), missing transverse energy $\not\!\!E_T$ (top right) after cut 1. The distribution of the azimuthal opening angle $\Delta\phi_{\mu\mu}$ after cut 1 (bottom left) and all cuts 1–5 (bottom right). The Higgs boson contribution is plotted for $M_H = 160\,\text{GeV}$. The Monte Carlo is normalized to the integrated luminosity in the data.

signal efficiencies for the three different channels after all cuts for six different Higgs boson masses.

IV. LIMITS ON THE CROSS SECTION $H \to WW^{(*)}$

The limit calculation was done following the method described in [13]. This method calculates the cross section limits at 95% C.L. with the integrated luminosity, number of background events, signal acceptance and number of events in data with corresponding errors as inputs. The uncertainty on the background was determined from the statistical and systematic error added in quadrature. The uncertainty on the luminosity is 6.5%. Table VII sums up the individual upper limits on the cross section times branching ratio for the three different decay channels for six different Higgs boson masses M_H. The different values of the upper limits for the three different channels especially for the two lowest mass points are a consequence of the different background contributions.

A combination of all three channels has been performed by multiplying the individual likelihood functions of all three channels resulting into a combined likelihood function. This is done separately for all six different masses. The cross-channel correlation given by the luminosity uncertainty and common object ID's in the different channels is

TABLE VII: Upper limits on the cross section times branching ratio for $\sigma \times BR(H \to WW)$ from the ee, $e\mu$, $\mu\mu$ final state and the combination of all three channels for different Higgs boson masses M_H.

M_H [GeV]	100	120	140	160	180	200
ee: limit $\sigma \times BR(H \to WW)$ [pb]	102.2	29.7	21.8	14.8	15.2	19.2
$e\mu$: limit $\sigma \times BR(H \to WW)$ [pb]	90.0	21.0	13.1	9.6	9.2	9.6
$\mu\mu$: limit $\sigma \times BR(H \to WW)$ [pb]	86.4	35.2	25.8	17.9	21.6	25.7
all: limit $\sigma \times BR(H \to WW)$ [pb]	40.1	12.0	8.2	5.7	5.8	6.6

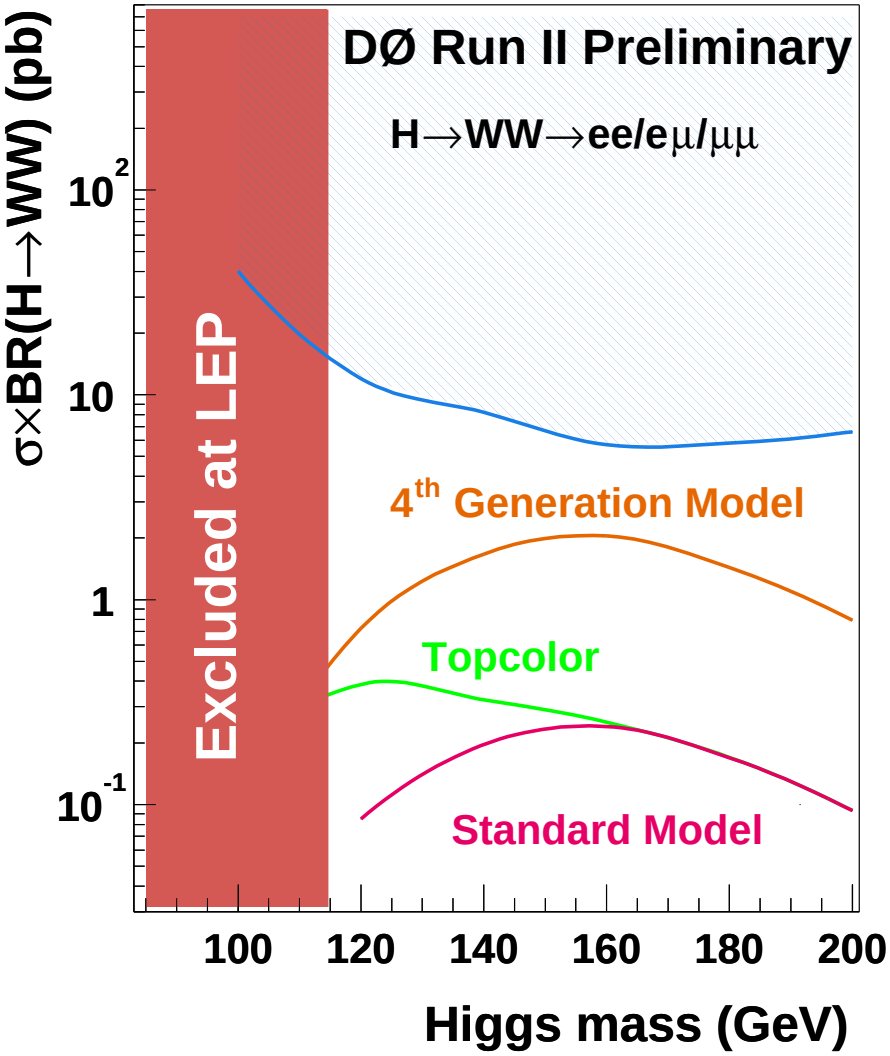

FIG. 4: Excluded cross section times branching ratio $\sigma \times BR(H \to WW^{(*)})$ at 95% C.L. together with expectations from standard model Higgs boson production and alternative models. The LEP limit on the standard model Higgs boson production is taken from [14], the 4th generation model is presented in [15], and the topcolor model is presented in [1].

determined to be small. Table VII shows the result of the combination. Figure 4 shows the calculated cross section limits for $\sigma \times BR(H \to WW^{(*)})$ for the different Higgs boson masses compared with predictions from the standard model and alternative models. The corresponding numbers are listed in Table VII.

V. CONCLUSIONS

A search for the process $H \to WW^{(*)} \to l^+\nu l'^-\bar{\nu}$ $(l = e, \mu)$ in $\mathcal{L} \approx 147 - 177\,\mathrm{pb}^{-1}$ of data recorded with the DØ experiment between April 2002 and September 2003 has been performed. After all cuts two events remain in data in both the ee and the $e\mu$ channel, while five events remain in the $\mu\mu$ channel, consistent with the standard model background expectations. Cross section limits for the combination of all channels have been calculated.

Acknowledgments

We thank the staffs at Fermilab and collaborating institutions, and acknowledge support from the Department of Energy and National Science Foundation (USA), Commissariat à L'Energie Atomique and CNRS/Institut National de Physique Nucléaire et de Physique des Particules (France), Ministry for Science and Technology and Ministry for Atomic Energy (Russia), CAPES, CNPq and FAPERJ (Brazil), Departments of Atomic Energy and Science and Education (India), Colciencias (Colombia), CONACyT (Mexico), Ministry of Education and KOSEF (Korea), CONICET and UBACyT (Argentina), The Foundation for Fundamental Research on Matter (The Netherlands), PPARC (United Kingdom), Ministry of Education (Czech Republic), Natural Sciences and Engineering Research Council and WestGrid Project (Canada), BMBF (Germany), A.P. Sloan Foundation, Civilian Research and Development Foundation, Research Corporation, Texas Advanced Research Program, and the Alexander von Humboldt Foundation.

[1] M. Carena *et al.* [Higgs Working Group Collaboration], "Report of the Tevatron Higgs working group", hep-ph/0010338.
[2] The DØ Collaboration, S.Abachi *et al.*, "The DØ Upgrade: The Detector and its Physics", Fermilab Pub-96/357-E (1996)
[3] M. Hohlfeld, "Search for the Higgs boson in $H \to WW^{(*)} \to e^+\nu e^-\bar{\nu}$ and $H \to WW^{(*)} \to e^\pm\nu\mu^\mp\nu$ decays", DØ Note 4392.
[4] J. Elmsheuser, "Search for the Higgs boson in $H \to WW^{(*)} \to \mu^+\nu\mu^-\bar{\nu}$ decays at DØ in Run II", DØ Note 4386.
[5] T. Sjostrand, P. Eden, C. Friberg, L. Lonnblad, G. Miu, S. Mrenna and E. Norrbin, Comput. Phys. Commun. 135 (2001) 238,hep-ph/0010017.
[6] M.L. Mangano, M. Moretti, F. Piccinini, R. Pittau, A. Polosa, JHEP 0307:001,2003, hep-ph/0206293.
[7] CTEQ Collab., H. L. Lai et al., Phys. Rev. D **55** 1280 (1997).
[8] A. Djouadi et al., Comp. Phys. Commun. 108 (1998) 56, hep-ph/9704448.
[9] M. Spira, Report DESY T-95-05 (October 1995), hep-ph/9510347.
[10] R. Hamberg, W. L. van Neerven and T. Matsuura, Nucl. Phys. **B359** 343 (1991) [Erratum-ibid. B 644 (2002) 403].
[11] J. M. Campbell and R. K. Ellis, Phys. Rev. D **60** 113006 (1999), hep-ph/9905386.
[12] The DØ Collaboration, V.M. Abazov *et al.*, Phys. Rev. D **67**, 012004 (2003).
[13] I. Bertram *et al.*, "A recipe for the Construction of Confidence Limits", Fermilab-TM-2104.
[14] The LEP Working Group for Higgs Boson Searches, *Search for the Standard Model Higgs Boson at LEP*, CERN-EP/2003-011.
[15] E. Arik, M. Arik, S. A. Cetin, T. Conka, A. Mailov and S. Sultansoy, Eur. Phys. J. C 26 (2002) 9, hep-ph/0109037.